

5-2011

Ocular Pathology Relevant to Glaucoma in a Gja1 (Jrt) Mouse Model of Human Oculodentodigital Dysplasia

Edmund Tsui
Western University

Kathleen A. Hill
Western University, khill22@uwo.ca

Alex M. Laliberte
Western University

Daniel Paluzzi
Western University

Ilia Kisilevksy
Western University

See next page for additional authors

Follow this and additional works at: <https://ir.lib.uwo.ca/anatomypub>

 Part of the [Anatomy Commons](#), and the [Cell and Developmental Biology Commons](#)

Citation of this paper:

Tsui, Edmund; Hill, Kathleen A.; Laliberte, Alex M.; Paluzzi, Daniel; Kisilevksy, Ilia; Shao, Qing; Heathcote, Godfrey J.; Laird, Dale W.; Kidder, Gerald M.; and Hutnik, Cindy M. L., "Ocular Pathology Relevant to Glaucoma in a Gja1 (Jrt) Mouse Model of Human Oculodentodigital Dysplasia" (2011). *Anatomy and Cell Biology Publications*. 57.
<https://ir.lib.uwo.ca/anatomypub/57>

Authors

Edmund Tsui, Kathleen A. Hill, Alex M. Laliberte, Daniel Paluzzi, Ilia Kisilevksy, Qing Shao, Godfrey J. Heathcote, Dale W. Laird, Gerald M. Kidder, and Cindy M. L. Hutnik

Ocular Pathology Relevant to Glaucoma in a *Gja1*^{Jrt/+} Mouse Model of Human Oculodentodigital Dysplasia

Edmund Tsui,¹ Kathleen A. Hill,² Alex M. Laliberte,² Daniel Paluzzi,² Ilia Kisilevsky,² Qing Shao,^{1,3} J. Godfrey Heathcote,⁴ Dale W. Laird,^{1,3} Gerald M. Kidder,^{1,5} and Cindy M. L. Hutnik⁶

PURPOSE. Oculodentodigital dysplasia (ODDD) is a human disorder caused by mutations in the gap junction alpha 1 (*GJA1*) gene encoding the connexin43 (Cx43) gap junction protein. Causal links between *GJA1* mutations and glaucoma are not understood. The purpose in this study was to examine the ocular phenotype for *Gja1*^{Jrt/+} mice harboring a Cx43 G60S mutation.

METHODS. In young *Gja1*^{Jrt/+} mice, Cx43 abundance was assessed with a Western blot, and Cx43 localization was visualized using immunohistochemistry and confocal microscopy. Intraocular pressure (IOP) was measured by rebound tonometry, and eye anatomy was imaged using ocular coherence tomography (OCT). Hematoxylin and eosin (H&E)-stained eye sections were examined for ocular histopathology related to the development of glaucoma.

RESULTS. Decreased Cx43 protein levels were evident in whole eyes from *Gja1*^{Jrt/+} mice compared with those of wild-type mice at postnatal day 1 ($P = 0.005$). Cx43 immunofluorescence in ciliary bodies of *Gja1*^{Jrt/+} mice was diffuse and intracellular, unlike the gap junction plaques prevalent in wild-type mice. IOP in *Gja1*^{Jrt/+} mice changed during postnatal development, with significantly lower IOP at 21 weeks of age in comparison to the IOP of wild-type eyes. Microphthalmia, enophthalmia, anterior angle closure, and reduced pupil diameter were observed in *Gja1*^{Jrt/+} mice at all ages examined. Ocular histology showed prominent separations between the pigmented and nonpigmented ciliary epithelium of *Gja1*^{Jrt/+} mice, split irides, and alterations in the number and distribution of nuclei in the retina.

CONCLUSIONS. Detailed phenotyping of *Gja1*^{Jrt/+} eyes offers a framework for elucidating human ODDD ocular disease mechanisms and evaluating new treatments designed to protect ocular synaptic network integrity. (*Invest Ophthalmol Vis Sci*. 2011;52:3539–3547) DOI:10.1167/iovs.10-6399

Oculodentodigital dysplasia (ODDD) is a rare, primarily autosomal dominant human disorder caused by any one of the 63 known mutations in the gap junction alpha 1 (*GJA1*) gene encoding the gap junction protein connexin43 (Cx43).^{1–2} It is characterized by syndactyly, loss of tooth enamel, and a wide range of ocular abnormalities.³ The ocular abnormalities reported for ODDD patients include microphthalmia, enophthalmia, microcorneas, malformations of the iris, elevated intraocular pressure (IOP), and glaucoma.^{3–5} Disease mechanisms leading to ODDD-related glaucoma are poorly understood, given the restrictions of purely associative data in human populations.

Cx43 forms an integral part of gap junctional intercellular communication through the formation of permeable channels between neighboring cells. Gap junctions are central to many important physiological processes in living organisms since they mediate cell-to-cell communication via small molecule and ion transfer.⁶ Cx43 is one of ~20 gap junction proteins that oligomerize to form hexameric connexons (gap junction hemichannels).⁷ Cx43 is the most widely expressed connexin, and Cx43 gap junctions are a major component of several structures in the eye, where they serve essential roles in cell homeostasis and nutrient transport.^{7,8} Within the eye, Cx43 is found in the corneal epithelium, ciliary body, lens, iris, and retina.⁷ Cx43 forms a large proportion of the gap junctions between the pigmented and nonpigmented epithelial cells in the ciliary body.⁷ These junctions are thought to be associated with the production of aqueous humor in the ciliary processes of the eye, which is relevant to maintenance of normal intraocular pressure and nourishment of the postnatal lens.⁹

A mutant mouse model (*Gja1*^{Jrt/+}) harboring a glycine-to-serine substitution at position 60 (G60S) in Cx43 was created through an *N*-ethyl-*N*-nitrosourea (ENU) mutagenesis screen and found to display a phenotype similar to human ODDD.¹⁰ There is reduced survivorship in *Gja1*^{Jrt/+} mice, with both prenatal and neonatal death.¹⁰ *Gja1*^{Jrt/+} mice exhibit the characteristic ODDD abnormalities of syndactyly and loss of tooth enamel. In addition, *Gja1*^{Jrt/+} mice display multiple craniofacial abnormalities including long narrow nose, depressed nasal bridge, and microcephaly.¹⁰ ODDD-like ocular abnormalities in *Gja1*^{Jrt/+} mice include microphthalmia, enophthalmia, corneal opacification, cataracts, abnormal pupil shape, aberrant pupillary light reflex, and iris malformations.¹⁰ Of the 20 connexins found in mice, Cx43 is the most ubiquitously expressed,¹¹ consistent with the wide array of tissues affected in the ODDD mutant mouse.

From the Departments of ¹Physiology and Pharmacology, ²Biology, and ³Anatomy and Cell Biology, The University of Western Ontario, London, Ontario, Canada; the ⁴Department of Pathology, Faculty of Medicine, Dalhousie University, Halifax, Nova Scotia, Canada; the ⁵Division of Genetics and Development, Children's Health Research Institute, London, Ontario, Canada; and the ⁶Department of Ophthalmology, Ivey Eye Institute, St. Joseph's Hospital, Lawson Health Research Institute, The University of Western Ontario, London, Ontario, Canada.

Supported by Canadian Institutes of Health Research Grant MOP 74637 (GMK, DWL); an infrastructure funding Grant RTI-1 from the Natural Sciences and Engineering Research Council (KAH); and the Department of Ophthalmology Pilot Fund at the University of Western Ontario for operation funding.

Submitted for publication August 12, 2010; revised October 19 and November 26, 2010; accepted December 6, 2010.

Disclosure: E. Tsui, None; K.A. Hill, None; A.M. Laliberte, None; D. Paluzzi, None; I. Kisilevsky, None; Q. Shao, None; J.G. Heathcote, None; D.W. Laird, None; G.M. Kidder, None; C.M.L. Hutnik, None

Corresponding author: Kathleen A. Hill, Department of Biology, The University of Western Ontario, London, Ontario, N6A 5B7, Canada; khill22@uwo.ca.

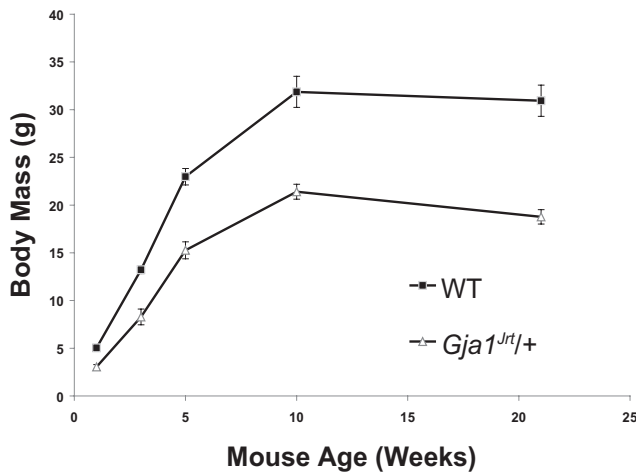


FIGURE 1. The *Gja1^{Jrt/+}* mice had significantly lower body mass (mean \pm SEM) compared with that of their wild-type (WT) littermates at 1 ($n = 5$ for both genotypes), 3 ($n = 8$ WT and 7 *Gja1^{Jrt/+}*), 5 ($n = 8$ for both genotypes), 10 ($n = 3$ WT and 4 *G60S*), and 21 weeks of age ($n = 3$ WT and 4 *Gja1^{Jrt/+}*). Significant differences were found for age $P < 0.01$, genotype $P < 0.01$ (ANOVA).

The ocular phenotype of *Gja1^{Jrt/+}* mice mimics aberrant features in the human ODDD eye, presenting an opportunity to study Cx43 relevance to eye structure and pathology, in particular with relevance to development of glaucoma. Our central hypothesis is that mutant Cx43 leads to loss of gap junctions, specifically in the ciliary body and iris where structural and functional integrity is lost, resulting in aberrations in aqueous fluid production and elevated intraocular pressure. Herein, Cx43 levels in the whole eye and in situ localization within the ciliary body were compared in *Gja1^{Jrt/+}* and wild-type littermates. Optical coherence tomography (OCT) was used to monitor, in vivo, the early development of ODDD ocular diseases. Tonometry was used to measure intraocular pressure (IOP). Finally, postmortem, ocular histology was assessed for the underlying mechanisms in the development of glaucoma.

MATERIALS AND METHODS

Mice

Gja1^{Jrt/+} mice were supplied by the Centre for Modeling Human Disease, University of Toronto, on a mixed C57BL/6j and C3H/HeJ background¹⁰ and were backcrossed to the C57BL/6 inbred strain for four generations. All mouse protocols were approved by The Animal Use Subcommittee of the University Council on Animal Care of the University of Western Ontario and adhered to the ARVO Statement for the Use of Animals in Ophthalmic and Vision Research. The mice were fed a standard diet in pellets or meal (Teklad Global 2018; Harlan PMI Foods, Mississauga, ON, Canada) and water ad libitum. The meal form of the diet was used for the mutant mice, given the enamel hypoplasia phenotype.¹² Room temperature was $21 \pm 1^\circ\text{C}$, with a relative humidity of 44% to 66%, and a 12-hour light/12-hour dark cycle. Body mass was recorded for all the mice at 1, 3, 5, 10, and 21 weeks of age. For in vivo measurements of IOP and OCT imaging of whole eye structure, the mice were anesthetized with a combination injection of ketamine (1.25 mg/10 g body weight) and xylazine (0.025 mg/10 g body weight). Body temperature was maintained throughout anesthesia with a circulating-water heating pad and an overhead heat lamp.

Western Blot Analysis of Ocular Cx43 Protein Levels

To determine the levels of Cx43 protein in the mouse eye, lysates were extracted from whole eyes of postnatal day 1 *Gja1^{Jrt/+}* ($n = 8$) and

wild-type ($n = 9$) mice by using a Triton-based extraction buffer containing 1% Triton-X 100, 10 mM Tris, 150 mM NaCl, 1 mM EDTA, 1 mM EGTA, 0.5% NP-40, 100 mM sodium fluoride, 100 mM sodium orthovanadate, and a protease inhibitor tablet (one tablet per 10 mL buffer; Roche, Laval, QC, Canada) at pH 7.4. Protein concentrations were measured using a BCA protein-determination kit (Thermo Scientific, Rockland, IL). Lysate samples (30 μg) were boiled for 5 minutes, subjected to 10% SDS-PAGE, and transferred to a nitrocellulose membrane. The membranes were blocked with 5% nonfat dry milk (Santa Cruz Biotechnology, Santa Cruz, CA) and 0.05% Tween 20 in PBS for 30 minutes at room temperature. Affinity-purified rabbit anti-Cx43 polyclonal (cat no. C6219; Sigma-Aldrich, St. Louis, MO) primary antibodies were incubated overnight at 4°C . The epitope used in the production of this antibody was a peptide corresponding to a C-terminal segment (amino acid residues 363-382) of the cytoplasmic domain of human/rat Cx43 with an additional N-terminal lysine. Anti-glyceraldehyde 3-phosphate dehydrogenase (GAPDH) antibodies (1:20,000; Chemicon/Millipore, Temecula, CA) were used in parallel, to assess gel loading. After washes with PBS-Tween 20, AlexaFluor 680 secondary antibodies (1:5000; A21076; Invitrogen, Burlington, ON, Canada) and IRDye 800 (1:5000; Rockland, Gilbertsville, PA) were used. Membranes were visualized with an infrared imaging system (Odyssey; LiCor, Lincoln, NE). Densitometry analysis of unsaturated images was performed with commercial software (Quantity ONE; Bio-Rad, Mississauga, ON, Canada) and protein levels were normalized to GAPDH.

Ocular Histology and Cx43 Localization

The enucleated eyes were fixed in a solution of 3.7% paraformaldehyde in phosphate-buffered saline (PBS) overnight at 4°C . The eyes were dehydrated, paraffin-embedded, and sectioned at 5 μm for hematoxylin and eosin (H&E) staining and Cx43 immunofluorescence assays. For H&E-

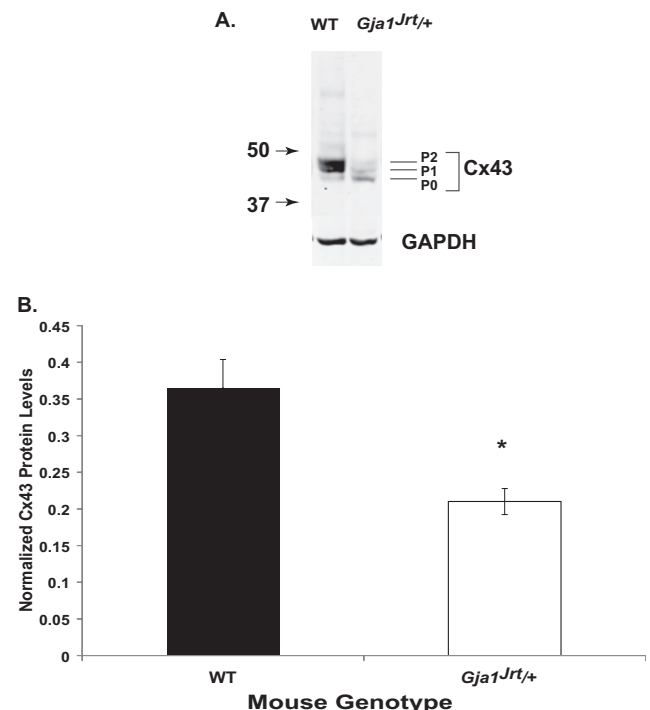


FIGURE 2. *Gja1^{Jrt/+}* mice had significantly lower levels of Cx43 protein. (A) Western blot and (B) densitometry analyses (mean \pm SEM) revealed decreased total Cx43 protein levels (includes non-phosphorylated P0, and phosphorylated Cx43 P1 and P2 species). Cx43 protein levels were assessed from whole eyes taken from P1 *Gja1^{Jrt/+}* mice ($n = 8$) and wild-type (WT) littermates ($n = 9$; $P < 0.005$, Student's *t*-test $P = 0.005$). Densitometry was performed, and total protein levels were normalized to GAPDH.

stained whole eye sections, cell density in the ganglion cell layer was determined for two 100- μm regions of the central retina and four regions of the peripheral retina. In these regions, the number of nuclei in the inner plexiform layer and the nuclear density of the ganglion cell layer were recorded. For Cx43 immunofluorescence (examined at 1, 3, and 5 weeks of age), slides were deparaffinized, treated with 2% bovine serum albumin (BSA), and treated with PBS for 1 hour at room temperature. The sections were incubated with polyclonal rabbit anti-Cx43 (as mentioned above; 1:200; Sigma Aldrich) for 1 hour at room temperature, followed by incubation with Alexa488 goat anti-rabbit antibody (1:300; Invitrogen) for 1 hour at room temperature. Tissue sections were then incubated with Hoechst 33342 stain (1:1000, Invitrogen) for 10 minutes at room temperature. Light and fluorescence microscopy images were captured (Veritas; Molecular Devices, Sunnyvale, CA) with magnifications from $\times 20$ to $\times 600$. Confocal microscopy was performed (LSM 5 Duo Vario; Carl Zeiss Meditec, Dublin, CA, with Zen software; Heidelberg Engineering, Heidelberg, Germany), and images were acquired at magnification $\times 630$, with zoom of 1.2. For blue (Hoechst 33342) fluorescence (diode 405-50), the settings were 1 AU, 362 master gain, 0.01 digital offset, and 3% laser intensity. Green (Alexa488) fluorescence (Argon 2 with laser lines 458, 477, 488, and 514) settings were 1 AU, 545 master gain, 0.01 digital offset,

and 7% laser intensity. The z-stacks were reconstructed and analyzed using the software to construct the 2D line profiles for Hoechst and/or Alexa488 fluorescence intensity.

IOP Measurements

IOP measurements were made in all the mice between 9 AM and 12 PM. Six successive IOP measurements were made in both eyes of each mouse (right and then left eye) with a rebound tonometer (Tonolab; TioLat, Helsinki, Finland), between 3 and 8 minutes after anesthesia. The highest and lowest IOPs for each eye were excluded, and the average of the remaining four measures was used as the IOP measure for each eye. IOP measurements were made for 3-, 5-, 10-, and 21-week-old *Gja1^{fl/fl}* and wild-type mice (minimum of $n = 3$ mice).

OCT Measurements

OCT was performed (Visante; Carl Zeiss Canada, Ltd., Toronto, ON, Canada), to image the anterior segment and retina of both eyes from 3-, 5-, and 10-week-old *Gja1^{fl/fl}* and wild-type mice (minimum of $n = 3$ mice). Diophenyl-T (Alcon, Mississauga, ON, Canada) was applied topically to achieve mydriasis. The high-resolution scan was centered at the vertex of

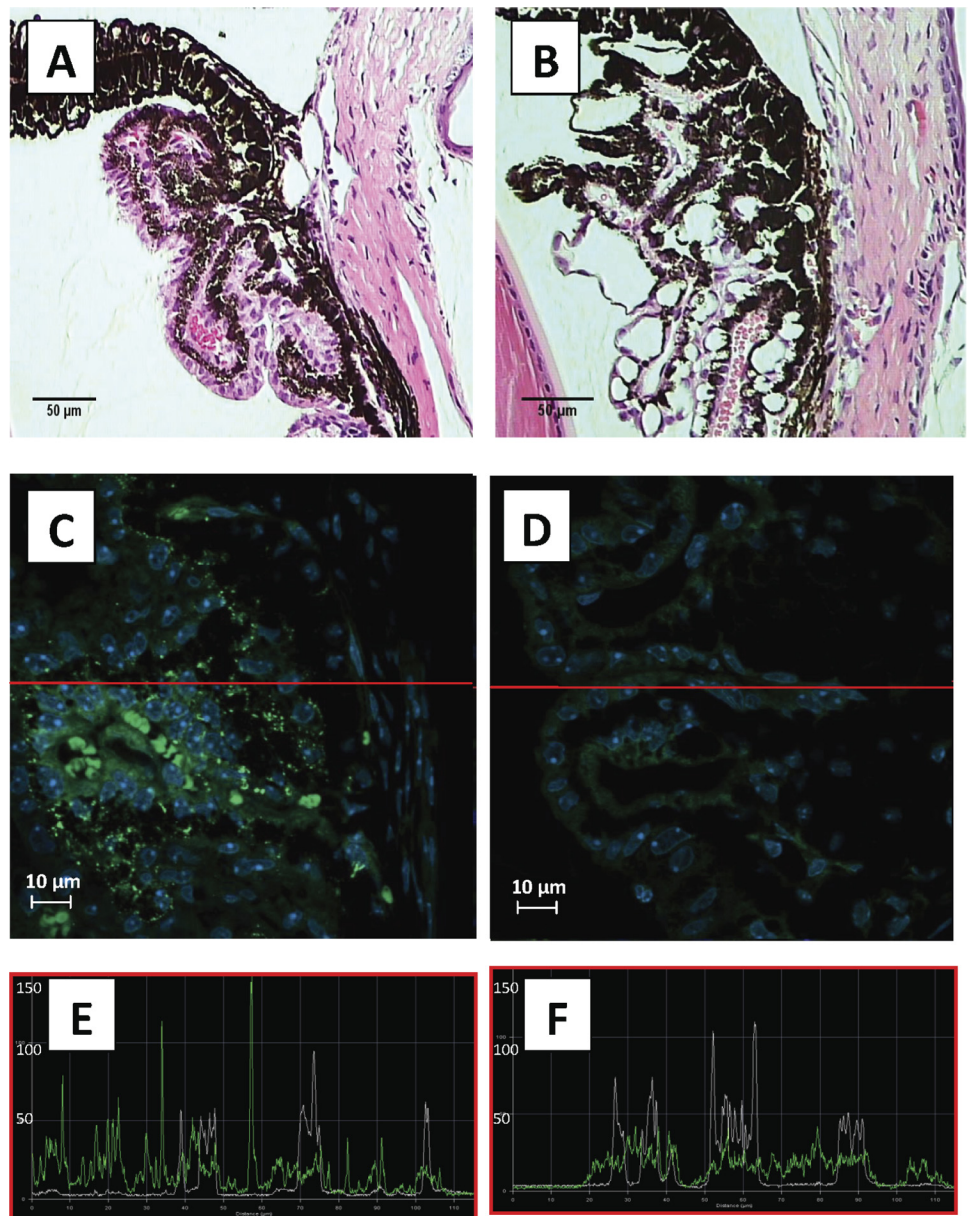


FIGURE 3. The ciliary bodies in the *Gja1^{fl/fl}* mice exhibited histopathology and altered Cx43 localization. H&E-stained cross sections of eyes from 5-week-old (A) WT mice and (B) *Gja1^{fl/fl}* littermates show prominent and numerous separations between the pigmented and nonpigmented epithelium of the ciliary epithelium, leaving clear vacuoles. (C) Cx43 immunofluorescence (green) was punctate, consistent with gap junction plaques and cell membrane localization in WT mice, compared with (D) diffuse and intracellular localization in the *Gja1^{fl/fl}* littermates at 3 and 5 weeks of age. Confocal imaging was performed with cryopreserved samples and thus was different from that of the H&E-stained sections. Nuclei are Hoechst stained (blue). See the Materials and Methods section for image settings. (C) Autofluorescence of peripheral erythrocytes was observed; (D) no peripheral erythrocytes were present. (C, D, red line) Position of the line graph data depicted in images (E) and (F). Line graphs show the results of semiquantitative analysis of fluorescence intensity across the ciliary process in (E) WT mice, compared with (F) *Gja1^{fl/fl}* littermates. The green and white spectra represent AlexaFluor and Hoechst stain intensity, respectively. Representative images of a 5-week-old mouse are shown. Magnification: (A, B) $\times 600$; (C, D) $\times 630$.

the mouse eye before image capture. Post-acquisition image analysis used a digital caliper tool in the system software to obtain the following measurements (in millimeters): anterior chamber width, anterior chamber depth, pupil diameter, central corneal thickness, and total neuronal retinal thickness. Anterior chamber angle was measured from the OCT images (ImageJ software; developed by Wayne Rasband, National Institutes of Health, Bethesda, MD; available at <http://rsb.info.nih.gov/ij/index.html>). The ratio of pupil diameter to anterior chamber width was also determined, to assess iris deformation standardized for eye size, given the significantly smaller eye size in *Gja1^{Jrt/+}* compared with wild-type mice. Data analysis was performed independently by two scorers, each blinded to the sample identifiers. After OCT, the mice were euthanized with an intraperitoneal injection of pentobarbital sodium (1.2 mg/10 g body weight), and both eyes were enucleated for postmortem analyses.

Statistical Analysis

Statistical analyses were performed with ANOVA and two-tailed Student's *t*-tests (Excel 2007 Microsoft, Redmond, WA, and SPSS, Chicago, IL). Significance was set at $P < 0.05$.

RESULTS

Lower Survivorship and Body Mass in *Gja1^{Jrt/+}* Mice

Mortality in the *Gja1^{Jrt/+}* mice was highest between 6 and 30 days of age (19% mortality for the male mice). The *Gja1^{Jrt/+}* mice compared with the wild-type littermates had significantly lower body mass at each age examined (Fig. 1; two-factor ANOVA $P = 0.001$). Average body mass was 60% to 39% lower than that of the wild-type mice from 1 to 21 weeks of age, respectively.

Lower Cx43 Protein Levels in Eyes of *Gja1^{Jrt/+}* Mice

Western blot analysis (Fig. 2A) revealed that Cx43 protein (including both phosphorylated and nonphosphorylated species) was present in whole eye lysates taken from the 1-day-old wild-type and mutant mice, but Cx43 levels were found to be significantly lower in the mutant mice (Fig. 2B). In particular, the levels of the slower migrating phosphorylated Cx43 species (P1 and P2) were greatly reduced in the mutant mice compared with that in the wild-type littermates.

Altered Ciliary Body Structure with Aberrant Cx43 Localization

In contrast to normal ciliary body structure (Fig. 3A; 5 weeks), prominent and numerous separations between pigmented epithelium and nonpigmented epithelium were observed in ciliary processes of each of the *Gja1^{Jrt/+}* mouse eyes at 3, 5, 10, and 21 weeks of age (Fig. 3B; 5 weeks). Qualitative analysis of Cx43 immunofluorescence in eyes from the 1-, 3-, and 5-week-old wild-type mice showed intense punctate staining consistent with the presence of Cx43 in gap junctions at cell-to-cell interfaces in the ciliary processes (Fig. 3C; 5 weeks). In contrast, immunofluorescence for Cx43 in the 1-, 3-, and 5-week-old *Gja1^{Jrt/+}* mice showed reduced punctate fluorescence with diffuse intracellular fluorescence (Fig. 3D; 5 weeks). These observations are consistent with an intracellular localization of Cx43 protein and decreased gap junction plaques in the ciliary processes. Quantitative evaluation of Cx43 localization in ciliary processes in the wild-type and *Gja1^{Jrt/+}* mice was performed with confocal microscopy (Figs. 3E, 3F), and these analyses revealed significant differences in the 2D spectra for Cx43 immunofluorescence intensity and location. Compared with the ciliary processes in the wild-type mice (Fig. 3E), Cx43 immunofluorescence in the *Gja1^{Jrt/+}* mice had significantly lower peak intensity and broader peak

areas, consistent with diffuse intracellular localization (Fig. 3F). Fluorescence peak intensity was less than 50 in the *Gja1^{Jrt/+}* mouse eyes but greater than 50 for the punctate gap junction plaques in the wild-type mouse eyes.

Gja1^{Jrt/+} Mice Have a Different IOP Profile with Age Compared to Wild-Type Mice

The profile of IOP with age differed significantly between the *Gja1^{Jrt/+}* and wild-type littermates ($P < 0.01$ for genotype and $P < 0.001$ for age and age and genotype interaction; ANOVA). IOP in the *Gja1^{Jrt/+}* mice was not elevated above the values observed in the wild-type littermates. IOP in the wild-type mice was relatively constant at 3 and 5 weeks of age and rose approximately 5.2 and 3.6 mm Hg by 10 and 21 weeks of age, respectively ($P < 0.001$; Fig. 4). IOP in the 3- and 10-week-old *Gja1^{Jrt/+}* mice was similar to that of the wild-type littermates. IOP in the *Gja1^{Jrt/+}* mice was significantly lower than that in the wild-type littermates at 5 weeks of age ($P < 0.001$). At 21 weeks of age, IOP in the *Gja1^{Jrt/+}* mice was 8.25 mm Hg below the average IOP of the wild-type eyes ($P < 0.001$). IOP in both eyes was similar in all study groups.

In Vivo Imaging Detects Structural Abnormalities in *Gja1^{Jrt/+}* Mouse Eyes

At all ages, the eyes of the *Gja1^{Jrt/+}* mice showed microphthalmia and enophthalmia on OCT images (Figs. 5B, 5D, 5F). OCT images clearly revealed elongated and split irides in the 5- and 10-week-old *Gja1^{Jrt/+}* mice (Figs. 5D, 5F). Quantitative analysis of OCT images revealed that the ratio of pupil diameter to anterior chamber width was significantly lower in the *Gja1^{Jrt/+}* mouse eyes (two-factor ANOVA; $P < 0.001$; Fig. 6A). The anterior chamber angle was smaller in the *Gja1^{Jrt/+}* mice compared with that in the wild-type mice at all ages (two-factor ANOVA; $P < 0.001$; Fig. 6B). The cornea and retina were thinner in the *Gja1^{Jrt/+}* mice compared with that in the wild-type mice, but overall eye size was smaller in the *Gja1^{Jrt/+}* mice. The cornea and retina of the *Gja1^{Jrt/+}* mice show parallel growth with age compared with that of the wild-type mice, with no evidence of corneal or retinal degeneration in the OCT images (Figs. 6C, 6D). Aberrant features were evident in both eyes of the same

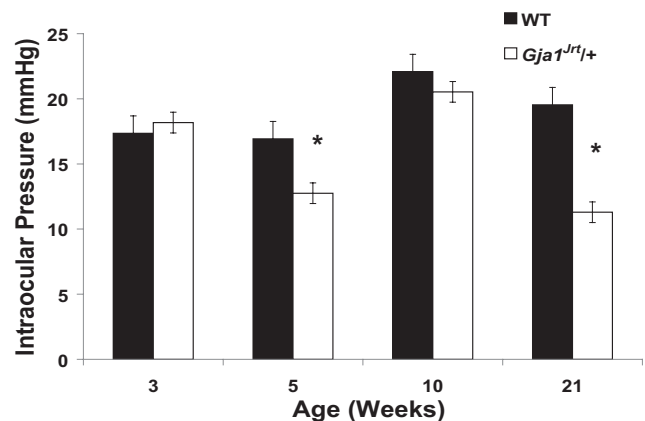


FIGURE 4. *Gja1^{Jrt/+}* and wild-type (WT) mice have different profiles of IOP with age. IOP measurements (mean \pm SEM for four replicates per eye) were made in *Gja1^{Jrt/+}* and WT mice at 3, 5, 10, and 21 weeks of age (minimum of three mice in each cohort). The profile of IOP with age in *Gja1^{Jrt/+}* mice compared with WT littermates was significantly different (ANOVA; $P < 0.01$ for genotype and $P < 0.001$ for age and age+genotype interaction). At 5 and 21 weeks of age, the *Gja1^{Jrt/+}* mice had significantly lower IOP compared with age-matched WT littermates ($P < 0.001$; ANOVA).

mouse, consistent with bilateral symmetry. The structural abnormalities observed with *in vivo* OCT imaging were comparable to the histologic evaluations made in H&E-stained whole eye cross sections postmortem.

Iris, Lens, and Retinal Abnormalities Are Evident in Histology Postmortem

The *Gja1^{Jrt/+}* mice had irides split into two layers that were evident as early as 1 week of age (Fig. 7B). The posterior

pigmented epithelium of the iris was adjacent to the anterior surface of the lens. Also, nuclear displacement from adjacent nuclear layers into the inner plexiform layer was prominent in the *Gja1^{Jrt/+}* mouse retinas at 5 weeks of age. The *Gja1^{Jrt/+}* mice had a significant reduction in the number of nuclei in the ganglion cell layer at 5 and 10 weeks of age ($P < 0.0001$; Fig. 7D). Ganglion nuclear counts in the peripheral and central retina of the *Gja1^{Jrt/+}* mice were 65% and 72% that of the wild-type mice. Ganglion cell loss and nuclear displacement

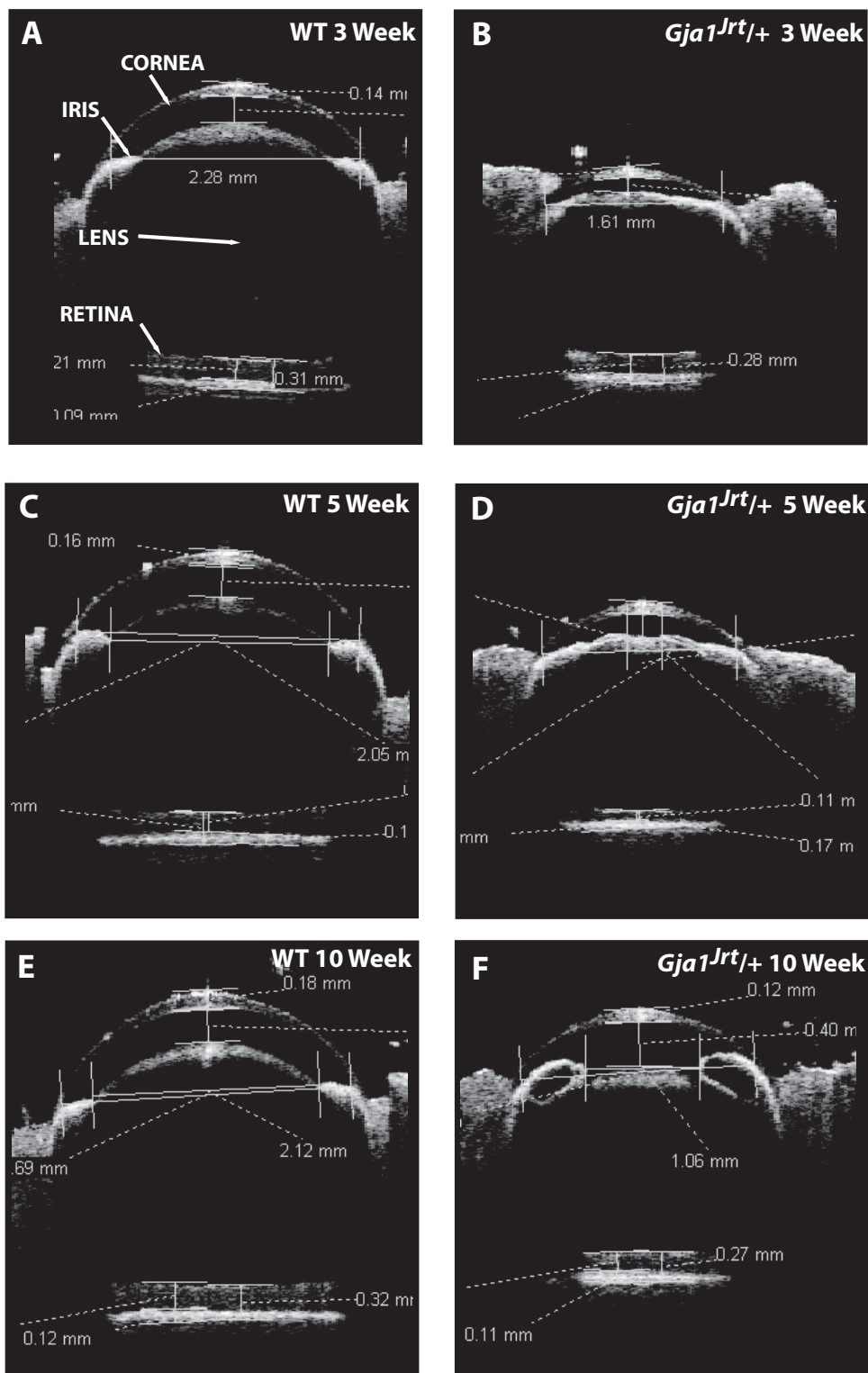


FIGURE 5. *In vivo* OCT of the anterior eye segment of the *Gja1^{Jrt/+}* mice reveals microphthalmia, enophthalmia, and split irises. Whole-eye anatomy was imaged for the wild-type (WT) compared with the *Gja1^{Jrt/+}* mice at (A, B) 3, (C, D) 5, and (E, F) 10 weeks of age.

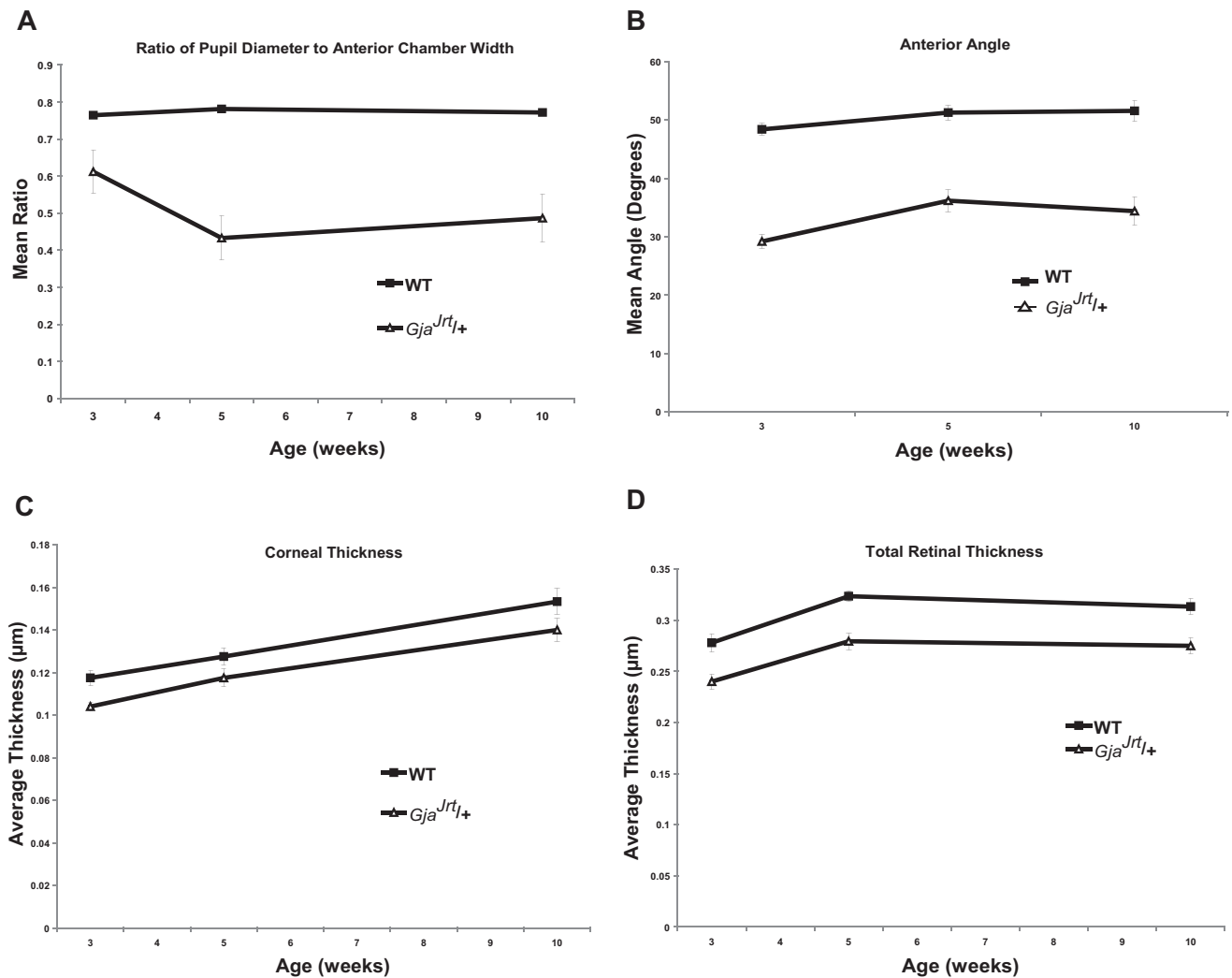


FIGURE 6. In vivo OCT revealed anterior segment and retinal structural abnormalities in *Gja1^{Jrt1+}* mice. (A) Ratio of the distance between the iris leaflets and the anterior chamber width was smaller in the *Gja1^{Jrt1+}* mice than in the wild-type (WT) mice ($P < 0.001$). (B) Anterior chamber angle was smaller in the *Gja1^{Jrt1+}* mice than in the WT mice ($P < 0.001$). The *Gja1^{Jrt1+}* mice compared with the WT mice had thinner (C) corneas and (D) retinas, but both tissues showed proportionate growth and no evidence of degeneration. (All measures are shown as the mean \pm SEM for a minimum of three mice in each cohort). No significant differences were found between left and right eyes, which is consistent with bilateral symmetry of these ocular features (data not shown).

were not evident in the eyes of the 21-week-old *Gja1^{Jrt1+}* mice. All eyes of the 21-week-old *Gja1^{Jrt1+}* mice showed a range of gross structural abnormalities (Fig. 8), including lens degradation (observed in one eye of a single mouse), optic nerve atrophy, and retinal disorganization and dysplasia. Solute precipitation was visible in the anterior and posterior chambers (Fig. 8).

DISCUSSION

Gja1^{Jrt1+} mice show iris adjacent to the lens consistent with a pupillary block mechanism of glaucoma. The IOP profile with age in the *Gja1^{Jrt1+}* mice differs from that observed in the wild-type mice, and the data support the hypothesis that this *GJA1* mutation has an effect on IOP. However, IOP in the *Gja1^{Jrt1+}* mice was not elevated above values observed in the wild-type littermates. In fact, at 21 weeks of age, decreased IOP in the *Gja1^{Jrt1+}* eyes was observed and can be attributed to the severely impaired aqueous fluid production consistent with the observed solute (protein) precipitation in intraocular spaces (Fig. 8). Consistent with these

observations, impaired aqueous fluid production was reported for a Cx43 conditional knockout mouse model.⁹ The precipitated protein is consistent with backflow from the episcleral venous plexus and the canal of Schlemm as a result of the low IOP.^{9,14} It is clear that the changes observed in the retina were not dependent on an elevated and sustained IOP. It is not clear how the fluctuations in IOP would contribute to the diversity of aberrations observed in the retina. The strongest correlate to later retinal aberrations is altered ciliary body and iris structure. The IOP profile may be consistent with observations and interest in humans that IOP fluctuation is an independent risk factor in glaucoma.^{15,16} The results could also suggest that non-IOP dependent factors weigh in more significantly in this model and may be worthy of pursuit for further investigation.

In addition to the functional relevance of Cx43 in anterior structure integrity, Cx43 is present in the lens⁹ and retina⁸ and contributes to the differentiation of retinal pigment epithelial cells.¹⁷ Lens histology appeared normal, with the exception of degradation evident in one eye from a single 21-week-old *Gja1^{Jrt1+}* mouse. The retinas of young

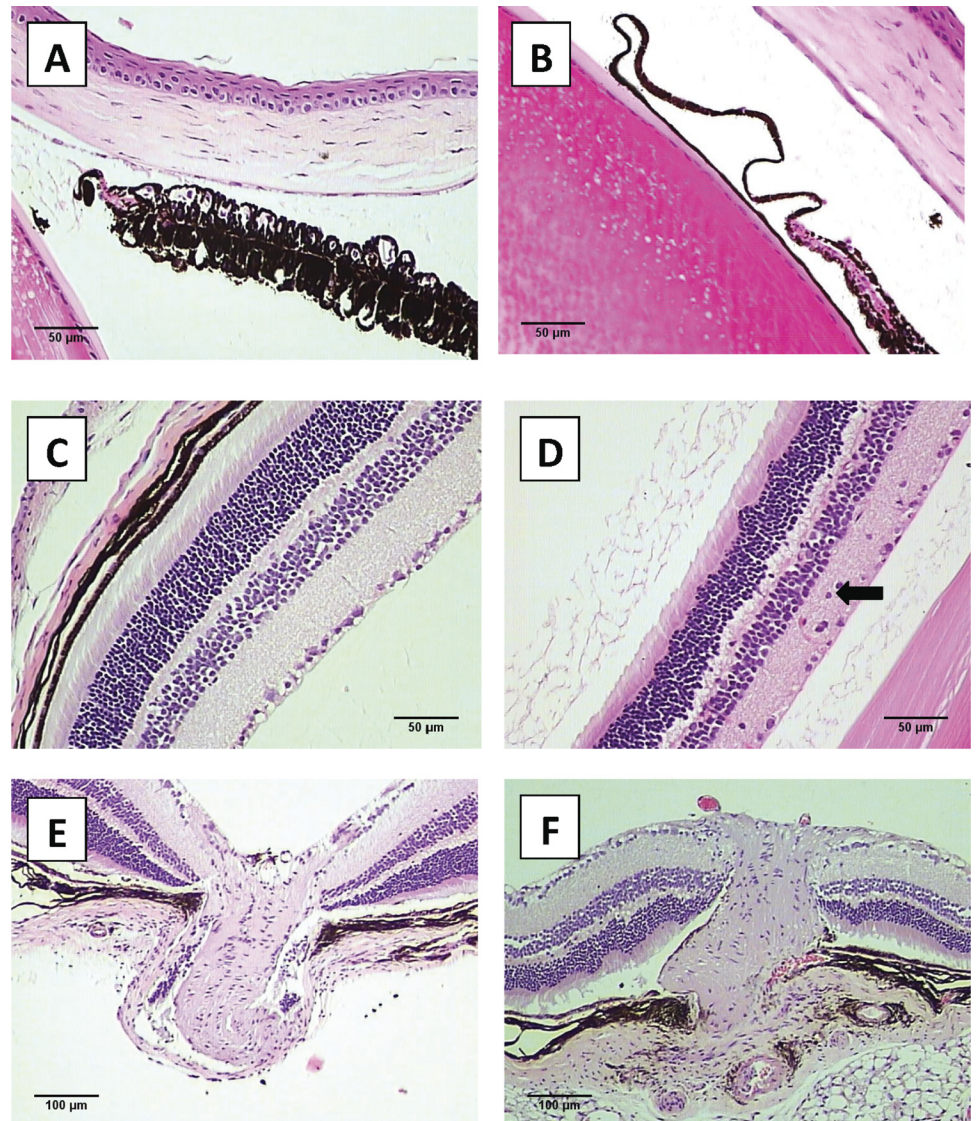


FIGURE 7. *Gja1^{prt/+}* eyes harbor multiple ocular histopathologies. Iris, retina, and optic nerve head histology was compared in 5-week-old wild-type (WT) and *Gja1^{prt/+}* mice (200 \times magnification; 5- μ m sections from formalin-fixed, paraffin-embedded whole eyes). (A) WT mice had normal iris histology. (B) The iris was split, leaving the posterior pigmented epithelium on the surface of the lens in *Gja1^{prt/+}* mice. Compared with (C) WT mice, (D) *Gja1^{prt/+}* mice had nuclei in the inner plexiform layer (arrow) and a lower density of ganglion cell layer nuclei. Histopathologies were evident at the earliest age examined (3 weeks). The optic nerve was examined in C-cut whole-eye sections for (E) normal histology in wild-type mice and (F) evidence of optic nerve histopathology in eyes from *Gja1^{prt/+}* mice.

Gja1^{prt/+} mice show diverse retinal changes, including a lower number of ganglion cell and nuclear displacements into the inner plexiform layer. These retinal histopathologies have been noted in other mouse models of retinal degeneration.¹⁸ There is some suggestion of shrinkage or loss of the prelaminar nerve substance at 10 weeks of age with early evidence of cupping of the optic disc, a clinical feature of human glaucoma,^{19,20} evident in eyes of 21-week-old *Gja1^{prt/+}* mice. The nature of this type of retinal degeneration is consistent with acute angle-closure glaucoma; however, the origin and progression of retinal disease in this mutant mouse is hypothesized to be the result of a complex interaction of compromised gap junction integrity in anterior structures (iris and ciliary epithelia) and the retina, including the retinal pigmented epithelium. Cases of ODDD in humans display various forms of glaucoma, including open- and closed-angle glaucoma with various IOP profiles and iris atrophy.^{2,4-5,21} The presence of retinal dysplasia in one 21-week-old *Gja1^{prt/+}* mouse indicates an element of abnormal formation as well as retinal degeneration.

The G60S amino acid substitution is at an evolutionarily conserved and hence functionally relevant amino acid in the first extracellular domain of Cx43.¹⁰ The G60S mutant shows a strong dominant-negative effect on endogenous wild-type

Cx43.^{10,22,23} The decreased number of gap junction plaques seen in the *Gja1^{prt/+}* ciliary processes has also been documented in other tissues of this mutant mouse such as the tooth enamel organ,¹² ovaries,²⁴ myometrium,²⁵ cardiomyocytes,¹⁰ heart ventricles,²⁶ and mammary gland,²⁷ all of which have been associated with impairments in the respective tissues. Also, *Gja1^{prt/+}* mouse cell culture studies have shown fewer Cx43 gap junctions and increased intracellular localization of Cx43 for neonatal cardiomyocytes²⁶ and granulosa cells.²⁴ Similarly, certain human Cx43 mutations have shown intracellular localization in cell culture assays.²²

Gja1^{prt/+} mice have an eye phenotype similar to mice with a conditional deletion in Cx43. Partial inactivation of Cx43 in the pigmented epithelium of the mouse ciliary processes by cre-loxP technology resulted in prominent vacuoles in the ciliary processes⁹ and reduced IOP in 5-week-old mice.²⁸ Cx43 gap junctions between the pigmented and the nonpigmented epithelium of the ciliary processes do not form properly and production of aqueous humor is reduced.^{28,29} This lack of Cx43 assembly into gap junctions is due to a trafficking defect that further results in aberrant or insufficient Cx43 phosphorylation.²⁴ Thus, the G60S Cx43 mutant acts dominantly on its co-expressed wild-type counterpart, consistent with that found in granulosa cells harvested from *Gja1^{prt/+}* mice.²⁴ Consis-

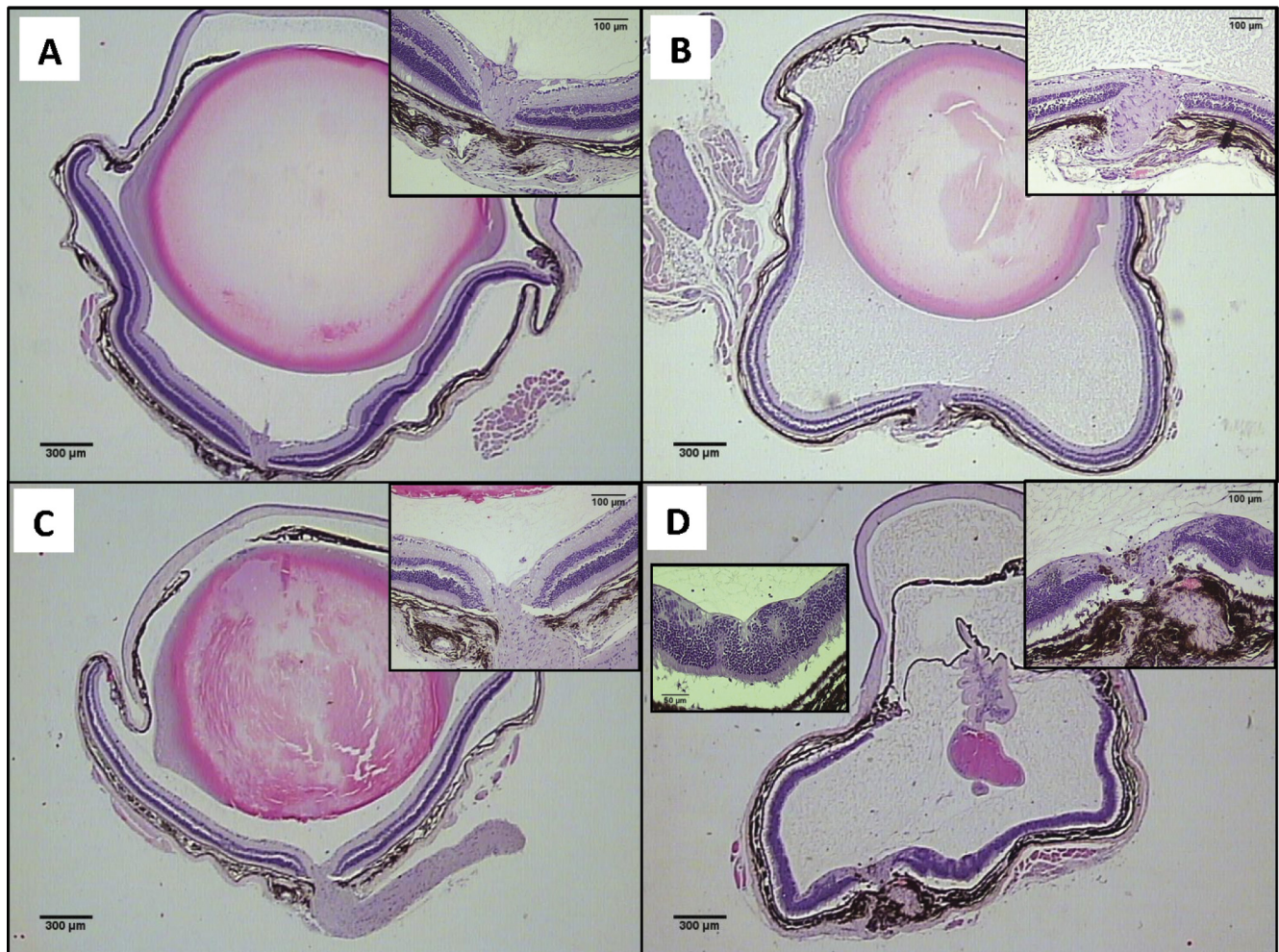


FIGURE 8. Structural abnormalities in eyes of 21-week-old G60S mice. The eyes of the *Gja1^{rt/+}* mice were severely deformed. Deviance from (A) wild-type (WT) eye normal histology was evident in moderate (B, C) to severe (D) disease phenotypes in *Gja1^{rt/+}* mice at 21 weeks of age. Structural abnormalities include evidence of early optic nerve head cupping (*insets*), retinal disorganization and dysplasia (D, *inset*), and lens atrophy. Solute precipitation in anterior and posterior chambers was evident in all *Gja1^{rt/+}* eyes. H&E-stained, paraffin-embedded sections; magnification: (A–D) $\times 20$; (*insets*) $\times 100$.

tently, in the heart, the G60S mutant protein is retained in the Golgi apparatus and appears to impair normal trafficking and function of co-expressed wild-type Cx43.²⁶

In addition to *Gja1^{rt/+}* mice, insertion of a conditional human Cx43^{G138R} mutation^{30,31} produced mutant mice with an ODDD-like ocular phenotype. The eye phenotype of a third ODDD-linked Cx43^{I130T} conditional mutant mouse has not been examined in detail. Similar to the other ODDD-linked mutant mice, Cx43^{I130T} mice harbor less phosphorylated Cx43 and exhibit impaired Cx43 trafficking to the cell surface.³² Further comparisons of the ocular phenotypes of mutant mice that mimic human ODDD will prove helpful in elucidating underlying disease mechanisms and dissecting the functionally relevant domains of Cx43 in the healthy eye.

CONCLUSIONS

Cx43 gap junctions are critical to the functional and structural integrity of epithelial tissues of the eye. A loss-of-function mutant of Cx43 is associated with altered cellular localization of Cx43 resulting in structural changes to ciliary body, iris, and retina evident in young mice. Structural deformations in the ciliary body and iris are hypothesized to alter trabecular meshwork integrity, closing trabecular beams and impeding aque-

ous fluid flow as a mechanism for a transitory increase in intraocular pressure in developing eyes of young mice. However, in adulthood, the underproduction of aqueous fluid by the ciliary body of *Gja1^{rt/+}* mice results in significantly lower IOP. Retinal degeneration (loss and displacement of neurons) and optic nerve degradation may reflect both degeneration as a result of the transient increase in IOP and aberrant histogenesis. Our results demonstrate the value of *in vivo* and postmortem ocular phenotyping of young *Gja1^{rt/+}* mice as a model to study synaptic pathophysiology. Our work represents the first characterization of the ocular features of a stable mutant model of ODDD, as well as the causative factors in ODDD-related retinal disease.

Acknowledgments

The authors thank Kevin Barr for lending his expertise in the maintenance of the mouse colony, Karen Nygard (Imaging and Data Analysis, The Biotron Experimental Climate Change Research Centre) for training in confocal microscopy, the personnel in the animal care facilities at The University of Western Ontario for providing resources and expertise, and the personnel at the Robarts Research Institute Molecular Pathology Facility for providing resources and expertise.

References

1. Paznekas WA, Karczeski B, Vermeer S, et al. GJA1 mutations, variants, and connexin 43 dysfunction as it relates to the oculodentodigital dysplasia phenotype. *Hum Mutat.* 2009;30:724-733.
2. Himi M, Fujimaki T, Yokoyama T, Fujiki K, Takizawa T, Murakami A. A case of oculodentodigital dysplasia syndrome with novel GJA1 gene mutation. *Jpn J Ophthalmol.* 2009;53:541-545.
3. Loddenkemper T, Grote K, Evers S, Oelerich M, Stogbauer F. Neurological manifestations of the oculodentodigital dysplasia syndrome. *J Neurol.* 2002;249:584-595.
4. Traboulsi EI, Parks MM. Glaucoma in oculo-dento-osseous dysplasia. *Am J Ophthalmol.* 1990;109:310-313.
5. Frasson M, Calixto N, Cronemberger S, de Aguiar RA, Leao LL, de Aguiar MJ. Oculodentodigital dysplasia: study of ophthalmological and clinical manifestations in three boys with probably autosomal recessive inheritance. *Ophthalmic Genet.* 2004;25:227-236.
6. Sohl G, Willecke K. An update on connexin genes and their nomenclature in mouse and man. *Cell Commun Adhes.* 2003;10:173-180.
7. Danesh-Meyer HV, Green CR. Focus on molecules: connexin 43—mind the gap. *Exp Eye Res.* 2008;87:494-495.
8. Kerr NM, Johnson CS, de Souza CF, et al. Immunolocalization of gap junction protein connexin43 (GJA1) in the human retina and optic nerve. *Invest Ophthalmol Vis Sci.* 2010;51:4028-4034.
9. Calera MR, Topley HL, Liao Y, Duling BR, Paul DL, Goodenough DA. Connexin43 is required for production of the aqueous humor in the murine eye. *J Cell Sci.* 2006;119:4510-4519.
10. Flenniken AM, Osborne LR, Anderson N, et al. A Gja1 missense mutation in a mouse model of oculodentodigital dysplasia. *Development.* 2005;132:4375-4386.
11. Evans WH, Martin PE. Gap junctions: structure and function (review). *Mol Membr Biol.* 2002;19:121-136.
12. Toth K, Shao Q, Lorentz R, Laird DW. Decreased levels of Cx43 gap junctions result in ameloblast dysregulation and enamel hypoplasia in Gja1Jrt⁺ mice. *J Cell Physiol.* 2010;223:601-609.
13. Laird DW, Puranam KL, Revel JP. Turnover and phosphorylation dynamics of connexin43 gap junction protein in cultured cardiac myocytes. *Biochem J.* 1991;273:67-72.
14. Raviola G. Blood-aqueous barrier can be circumvented by lowering intraocular pressure. *Proc Natl Acad Sci U S A.* 1976;73:638-642.
15. Detry-Morel M. Currents on target intraocular pressure and intraocular pressure fluctuations in glaucoma management. *Bull Soc Belge Ophthalmol.* 2008;(308):35-43.
16. Sultan MB, Mansberger SL, Lee PP. Understanding the importance of IOP variables in glaucoma: a systematic review. *Surv Ophthalmol.* 2009;54:643-662.
17. Kojima A, Nakahama K, Ohno-Matsui K, et al. Connexin 43 contributes to differentiation of retinal pigment epithelial cells via cyclic AMP signaling. *Biochem Biophys Res Commun.* 2008;366:532-538.
18. Richter M, Gottanka J, May CA, Welge-Lüssen U, Berger W, Lutjen-Drecoll E. Retinal vasculature changes in Norrie disease mice. *Invest Ophthalmol Vis Sci.* 1998;39:2450-2457.
19. Knox DL, Eagle RC Jr, Green WR. Optic nerve hydropic axonal degeneration and blocked retrograde axoplasmic transport: histopathologic features in human high-pressure secondary glaucoma. *Arch Ophthalmol.* 2007;125:347-353.
20. Greenfield DS, Siatkowski RM, Glaser JS, Schatz NJ, Parrish RK 2nd. The cupped disc: who needs neuroimaging? *Ophthalmology.* 1998;105:1866-1874.
21. Vasconcellos JP, Melo MB, Schimiti RB, Bressanim NC, Costa FF, Costa VP. A novel mutation in the GJA1 gene in a family with oculodentodigital dysplasia. *Arch Ophthalmol.* 2005;123:1422-1426.
22. McLachlan E, Manias JL, Gong XQ, et al. Functional characterization of oculodentodigital dysplasia-associated Cx43 mutants. *Cell Commun Adhes.* 2005;12:279-292.
23. Roscoe W, Veitch GI, Gong XQ, et al. Oculodentodigital dysplasia-causing connexin43 mutants are non-functional and exhibit dominant effects on wild-type connexin43. *J Biol Chem.* 2005;280:11458-11466.
24. Tong D, Colley D, Thoo R, et al. Oogenesis defects in a mutant mouse model of oculodentodigital dysplasia. *Dis Model Mech.* 2009;2:157-167.
25. Tong D, Lu X, Wang HX, et al. A dominant loss-of-function GJA1 (Cx43) mutant impairs parturition in the mouse. *Biol Reprod.* 2009;80:1099-1106.
26. Manias JL, Plante I, Gong XQ, et al. Fate of connexin43 in cardiac tissue harbouring a disease-linked connexin43 mutant. *Cardiovasc Res.* 2008;80:385-395.
27. Plante I, Laird DW. Decreased levels of connexin43 result in impaired development of the mammary gland in a mouse model of oculodentodigital dysplasia. *Dev Biol.* 2008;318:312-322.
28. Calera MR, Wang Z, Sanchez-Olea R, Paul DL, Civan MM, Goodenough DA. Depression of intraocular pressure following inactivation of connexin43 in the nonpigmented epithelium of the ciliary body. *Invest Ophthalmol Vis Sci.* 2009;50:2185-2193.
29. Coffey KL, Krushinsky A, Green CR, Donaldson PJ. Molecular profiling and cellular localization of connexin isoforms in the rat ciliary epithelium. *Exp Eye Res.* 2002;75:9-21.
30. Dobrowolski R, Sasse P, Schrickel JW, et al. The conditional connexin43G138R mouse mutant represents a new model of hereditary oculodentodigital dysplasia in humans. *Hum Mol Genet.* 2008;17:539-554.
31. Dobrowolski R, Hertig G, Lechner H, et al. Loss of connexin43-mediated gap junctional coupling in the mesenchyme of limb buds leads to altered expression of morphogens in mice. *Hum Mol Genet.* 2009;18:2899-2911.
32. Kalcheva N, Qu J, Sandeep N, et al. Gap junction remodeling and cardiac arrhythmogenesis in a murine model of oculodentodigital dysplasia. *Proc Natl Acad Sci U S A.* 2007;104:20512-20516.